Stress Waves in Rocks and their Effects on Rock Breakage

By

Ichiro Ito*, Makoto Terada* and Takehisa Sakurai†

In these experimental studies the authors have chiefly investigated the characteristics of the stress waves in rocks caused by detonators or explosives. The research consisted of two parts.

In the first part, we have treated mainly the phenomena which accompany the detonator's attack and have discussed the dynamic characteristics of rocks under such impulsive loadings. The following results were obtained from this part of the investigation.

The values of Young's moduli for rocks obtained dynamically are about two or three times greater than those obtained statically. The dynamic strengths of rocks are also greater than the static ones, but the difference seems to be not so great as in the case of metals. Moreover, it is an interesting result that various shock effects appear in accordance with the physical properties of rocks.

In the second part we advanced to a study of the phenomena accompanying an explosive's attack and observed chiefly the changes in the propagation velocities of the induced stress waves near the explosion point. The results obtained can be summarized as follows.

From the results obtained concerning the changes in the velocity of propagation of the stress waves with distance, a plastic wave of higher order seems to exist in the region very near the point of explosion and the appearance of the plastic wave seems to depend not only on the physical characteristics of the rocks but also on the brisance of the explosives. The compressibility of a rock under impulsive high pressure is peculiar to the physical properties of the rock, and it has no relation to the natures of the explosive. The peak pressure of the wave front decreases very rapidly with distance, and only within a few centimeters of the point of explosion do the explosives develop a different high pressure in proportion to their brisances.

Introduction

In industrial blasting, the objects blasted are generally providential rocks, and the effects of blasting are influenced by the characteristics of the explosives used as well as by the conditions of blasting adopted, so it is considerably difficult to observe the phenomena of blasting exactly and to analyse them in detail.

In general the breakage of a material is influenced not only by the spacial

---

* Department of Mining Engineering
† Taketoyo Factory, Nihon Yushi Co., Ltd.

distribution of the internal stresses caused by the load imposed upon it but also by the method of loading; in other words whether it is statically loaded, or alternately loaded, or suddenly and undulatingly loaded.

In blasting operations, the rocks are supposed to be fractured at first by the instantaneous severe shock effects caused by the detonation of explosives and then broken by the subsequent quasi-statical propulsion effects of the expanding gases.

Therefore, to understand thoroughly the phenomena of blasting and also to consider the mechanism of rock breakage by blasting, it is quite important to make clear the dynamic characteristics of rocks for these undulating alternate loads caused by the detonation of explosives.

But little research has been done to study these dynamic characteristics of rocks except when the rocks have been subjected to impulsive loadings at low speed.

Consequently, the authors have carried out a few experimental studies in order to investigate the characteristics of the stress waves induced in rocks when they are attacked by detonators or by explosives and also to study the relationship between these wave motions and the breakage of rocks.

General Principles

Generally when a cylindrical bar specimen is struck at one end by some impulsive loading, a compressional stress wave is generated and propagated along the axis of the bar. In this case it is well known that the stress at any point in the bar specimen can be represented by the following equation (1), provided that the wavelength of the stress wave is long compared with the diameter of the specimen, in other words when the wave is assumed to be a perfectly plane elastic one[1] :

$$\sigma = \rho c_0 v \qquad\qquad (1)$$

where σ is the stress, ρ is the density, c_0 is the velocity of propagation of the stress wave, and v is the particle velocity.

Consequently, if we can measure the values of c_0 and v, we can calculate the stress which is acting along the direction of the propagation of the wave.

To obtain the velocity of propagation of the induced stress wave, a method was used which measured the time required for the stress wave to propagate between two known marks on the specimen. In order to measure the particle velocity, methods similar to the ones used by Rinehart and others[2] were utilized in our experiments.

Stress Waves Induced in Rook Specimens Attacked by Detonators

The general arrangement of the experimental apparatus for the series of experiments in which detonators were used to strike the specimen, is shown in Fig. 1.
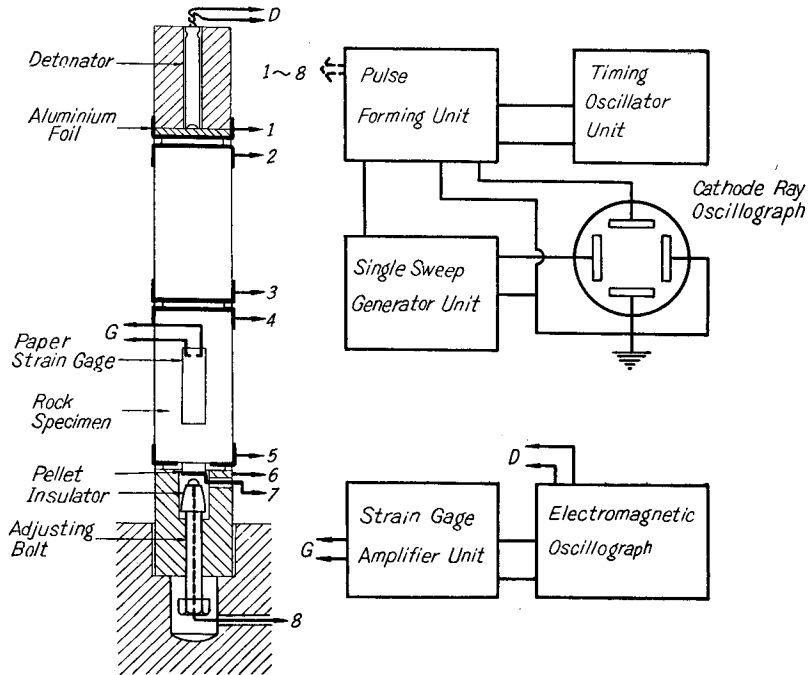

Fig. 1. General experimental arrangement.

An upper steel cylinder in which a detonator is placed along its axis, a marble cylinder, a rock specimen and a lower steel cylinder in which an adjusting bolt is installed, are piled up one upon another. The ends of these cylinders are smoothly polished and aluminium foil is cemented on each end to form an electric contact. An insulating paper 3/100 mm thick is inserted between each electric contact piece. A marble cylinder placed between the upper steel cylinder and the rock specimen is inserted in order to adjust the lag of the trigger of the sweep which is expected to occur until the first pulse caused by the explosion of the detonator appears.

A small pellet, which is made from the same rock as the specimen and is covered with aluminium foil at one end, is attached to the lower surface of the rock specimen with a thin film of grease and introduced into the notch in the centre of the upper end of the lower steel cylinder. The above four parts are fastened tightly together by means of scotch tape so as not to change the mutual relations.

Then the distance between the two electric contact pieces, one at the top of the bolt and the other the aluminium foil at the lower end of the pellet, is adjusted until exactly equal to a predetermined length.

Consequently, in this arrangement, the sets of electric contacts are intended to play the following roles:

(1) 1 and 2 are to start the single sweep of the cathode ray oscillograph through the trigger circuit.

(2) 3 and 4 are to mark the first pulse which designates the arrival of the stress wave at the upper end of the rock specimen.

(3) 5 and 6 are to mark the second pulse which designates the arrival of the stress wave at the lower end of the rock specimen.

(4) 7 and 8 are to mark the third pulse which designates the moment of the arrival of the pellet at the top of the bolt after flying a definite distance from the lower end of the specimen.

All records were taken with cathode ray oscillograph units. An example of these records is shown in Fig. 2.
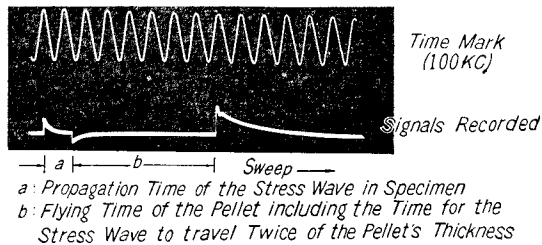

a : Propagation Time of the Stress Wave in Specimen
b : Flying Time of the Pellet including the Time for the
    Stress Wave to travel Twice of the Pellet's Thickness

Fig. 2.   An example of the oscillograms.

The time required for the stress wave to travel in the specimen and for the pellet to fly a definite distance can be measured from these records, and the velocity of propagation of the stress wave in the specimen and also the velocity of the flying pellet can be calculated from them. In these experiments, the velocity of the flying pellet was considered to be identical with the particle velocity at the lower end of the rock specimen. But as the particle velocity calculated in this way is the mean velocity for each thickness of the pellet, it is necessary to re-arrange it for the mean local velocity for each unit spacing.

Thus we can obtain the values of c_0 and v.

The strains in the rock specimen associated with these impulsive loadings were measured by using electric resistance strain gages, amplifiers and an electro-magnetic oscillograph. For the electric resistance strain gage, a paper type gage of which the gage factor was 2.03 and the electric resistance was 120 ohms was chosen, and it was always cemented at the centre of the cylindrical surface of the specimen. The vibrators installed in the oscillograph were of a type with a natural frequency of 6,000 c.p.s. and a sensitivity of 2 mA/mm. An example of these strain records is shown in Fig. 3.

The rock specimens were made of Mine marble from Yamaguchi prefecture and Izumi sandstone from Osaka prefecture, all in the definite size of 25 mm in diameter and 50 mm in length.

$\vdash$————$\frac{1}{120}$ sec————$\dashv$ ◾ *Time Mark*
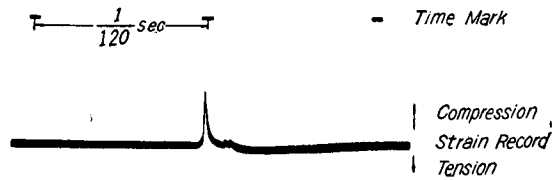
Compression
Strain Record
Tension

Fig. 3. An example of the strain records.

Moreover, in the case of the sandstone specimens, care was taken so that the axis of the specimen was parallel to the direction of its bedding plane.

To study the phenomena under various intensities of explosion, several classes of electric detonators, from No. 1 to No. 8, were used separately.

The results obtained for the measurements of the mean propagation velocity of the stress wave are shown in Table 1. The densities measured were 2.70 g/cm³ for marble and 2.60 g/cm³ for sandstone.

The particle velocities which were calculated directly from the results of the measurements of the flying velocities of the pellets are shown in Figs. 4 and 5.
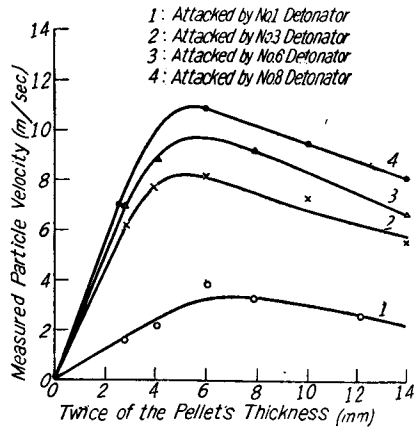
1 : Attacked by No.1 Detonator
2 : Attacked by No.3 Detonator
3 : Attacked by No.6 Detonator
4 : Attacked by No.8 Detonator

Fig. 4. Measured particle velocities for marble.

1 : Attacked by No.5 Detonator *
2 : Attacked by No.3 Detonator
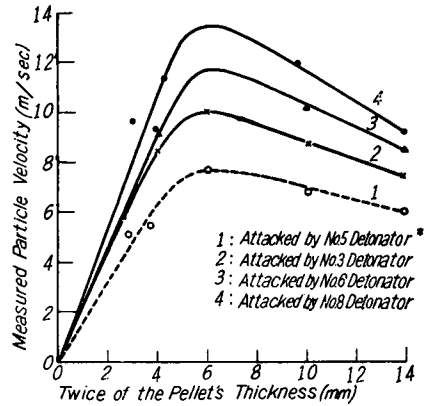3 : Attacked by No.6 Detonator
4 : Attacked by No.8 Detonator

Fig. 5. Measured particle velocities for sandstone.

* In this case the length of the marble cylinder used to adjust the lag of the trigger of the sweep was 100 mm, while in the other cases it was all arranged to a definite length of 50 mm.

Table 1. Propagation Velocities of the Stress Waves Measured

Detonator used	Propagation Velocity (m/sec)		Remarks
	in Marble	in Sandstone	
No. 1†	1,860	—	† Length of the cylindrical marble used to adjust the lag of the trigger of the sweep was 50 mm.
No. 3†	2,300	2,840	
No. 5*	—	2,300	
No. 6†	3,170	2,880	* Length of the cylindrical marble used to adjust the lag of the trigger of the sweep was 100 mm.
No. 8†	3,330	3,000	

Table 2. Summarized Results of Experiments

(A) Marble

Detonator used	Twice Thickness of Pellet (mm)	Particle Velocity (m/sec)		Time for Stress Wave to Propagate (μ sec)	Calculated Stress (kg/cm²)
		Measured Velocity	Rearranged Local Velocity		
No. 1	0	—		—	
			1.20		61.6
	2	1.20		1.08	
			3.74		192.0
	4	2.48		2.15	
			4.95		254.0
	6	3.30		3.23	
			3.42		175.0
	8	3.35		4.30	
			1.84		94.0
	10	3.00		5.38	
			1.16		59.7
	12	2.72		6.45	
			0.68		35.0
	14	2.44		7.53	
No. 3	0	—		—	
			4.55		324
	2	4.55		0.88	
			10.80		770
	4	7.70		1.75	
			9.05		645
	6	8.15		2.63	
			5.55		395
	8	7.50		3.50	
			4.25		303
	10	6.85		4.38	
			3.30		235
	12	6.30		5.25	
			2.80		200
	14	5.80		6.13	
No. 6	0	—		—	
			5.10		445
	2	5.10		0.63	
			12.30		1,074
	4	8.80		1.26	
			11.70		1,022
	6	9.75		1.90	
			8.25		720
	8	9.25		2.53	
			5.90		515
	10	8.45		3.16	
			4.25		370
	12	7.60		3.79	
			3.10		270
	14	6.70		4.42	
No. 8	0	—		—	
			5.60		514
	2	5.60		0.62	
			16.00		1,470
	4	10.00		1.24	
			12.95		1,190
	6	10.85		1.87	
			9.05		830
	8	10.20		2.49	
			6.75		620
	10	9.50		3.11	
			5.00		458
	12	8.80		3.73	
			3.50		320
	14	8.10		4.35	

(B) Sandstone

Detonator used	Twice Thickness of Pellet (mm)	Particle Velocity (m/sec)		Time for Stress Wave to Propagate (μ sec)	Calculated Stress (kg/cm^2)
		Measured Velocity	Rearranged Local Velocity		
No. 5	0	—	3.20	—	195
	2	3.20	9.40	0.87	574
	4	6.40	10.30	1.74	629
	6	7.70	6.90	2.61	422
	8	7.54	5.15	3.48	314
	10	7.05	4.00	4.35	244
	12	6.50	3.00	5.22	183
	14	6.00		6.09	
No. 3	0	—	4.20	—	317
	2	4.20	12.30	0.71	920
	4	8.48	13.00	1.41	975
	6	10.05	8.40	2.12	633
	8	9.50	5.60	2.82	422
	10	8.72	3.40	3.53	256
	12	8.08	1.60	4.24	121
	14	7.40		4.94	
No. 6	0	—	4.50	—	342
	2	4.50	13.70	0.70	1,040
	4	9.10	16.90	1.40	1,280
	6	11.70	10.30	2.10	780
	8	11.25	6.70	2.80	508
	10	10.30	4.25	3.50	322
	12	9.40	2.20	4.20	167
	14	8.50		4.90	
No. 8	0	—	5.40	—	430
	2	5.40	16.40	0.67	1,305
	4	10.90	18.70	1.33	1,490
	6	13.50	10.80	2.01	860
	8	12.85	7.20	2.67	574
	10	11.65	4.60	3.34	367
	12	10.45	2.50	4.02	199
	14	9.20		4.67	

From these results, the particle velocities for each thickness of pellet were re-arranged to obtain the mean local velocities for each unit spacing.

Then the stresses at the lower end of the rock specimen were calculated. These results are shown in block in Table 2.

The stress wave shapes in the rock specimen thus obtained are shown in Figs. 6 and 7. As shown in these figures, the stress waves in these cases were characterized by an instantaneous rapid rise of the stress and a comparatively slower fall of the stress, although they took somewhat different shapes in accordance with the strength of the detonator used.
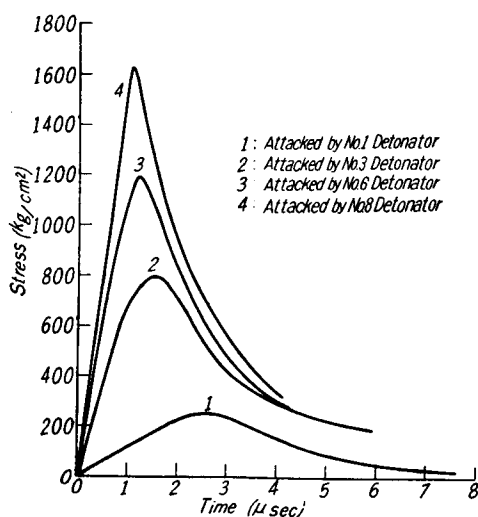
Fig. 6. Stress wave shapes for marble.   Fig. 7. Stress wave shapes for sandstone.
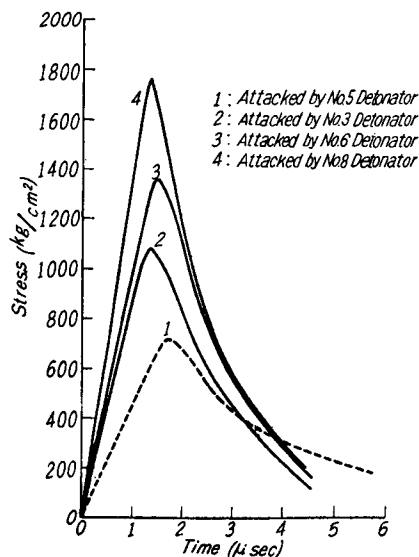
The relationship between the dynamic stress and strain can be traced assuming that the maximum dynamic stress corresponds approximately to the maximum dynamic strain in the specimen observed simultaneously in each case of the measurements. The results thus obtained were compared with the statical stress-strain relationship in Figs. 8 and 9, where the statical values were determined by statical compression tests in a testing machine.

From these figures it is clear that the dynamic Young's modulus of the rock specimens is somewhat greater than the static one as shown in Table 3. More-over, these dynamic situations of the rocks are fairly different from those obtained in the case of metals and polythenes. In the latter cases, as has been pointed out by H. Kolsky[3] and others (Fig. 10), the phenomena of so-called plastic flow occurs when the stress in the material reaches to a high value which greatly exceeds its own elastic limit. But in the case of the rock specimens, at least so
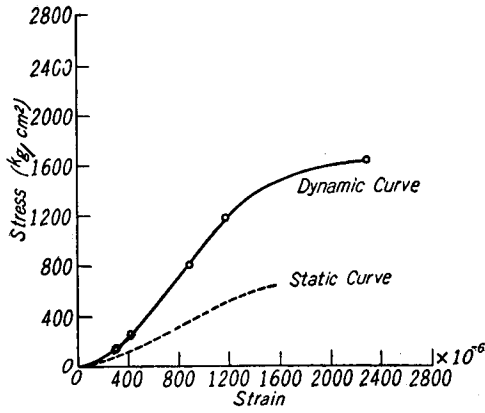
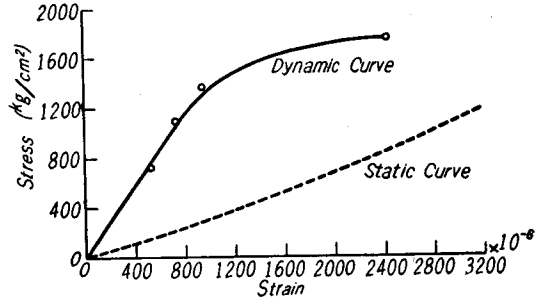Fig. 8. Dynamic and static stress-strain diagram for marble.

Fig. 9. Dynamic and static stress-strain diagram for sandstone.

Table 3 Dynamic and Static Young's Moduli of Rocks Tested

Kind of Rocks	Dynamic Young's Modulus, Ed (kg/cm²)	Static Young's Modulus, Es (kg/cm²)	Ed/Es
Marble	12.6×10^5	5.3×10^5	2.38
Sandstone	13.1×10^5	3.5×10^5	3.74
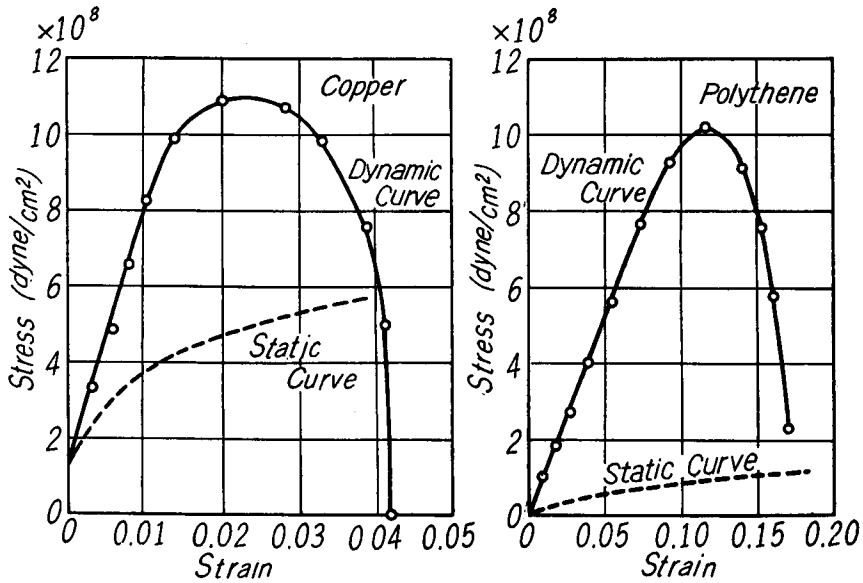
Fig. 10. Dynamic and static stress-strain diagrams for copper and polythene. (After H. Kolsky).

far as the present experiments with the detonators are concerned, definite plastic flow could not be observed, and the rocks appeared to undergo brittle fractures when the dynamic stress in them exceeded certain high values above their own elastic limits. However, with reference to plastic flow observed in rock specimens, consideration must be given to the results of the later experiments with explosives.

The appearance of the rock specimens after experiments did not differ greatly from the virgin specimens, but for the specimens attacked by No. 8 detonators, it was observed that some aspects of the individual particles in the crystalline structure were partially altered, although definite cracks could not be observed. For trial, compression tests using the testing machine of the Amsler type were carried out with the specimens attacked by detonators and the results were compared with those obtained for the virgin specimens. Fig. 11 shows the stress-strain relations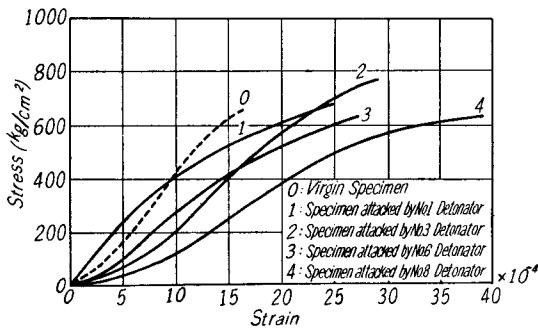hip for the marble specimens thus obtained, and it is interesting to note that in these cases some invisible changes in the nature of the marble specimen have been caused by the detonator's attacks. Generally Young's moduli for specimens attacked by detonators are somewhat less than those of the virgin specimens, and this tendency is notable in accordance with an increase in the intensity of the impulsive loadings. On the contrary, as shown in Fig. 12, the sandstone specimens did not show any substantial changes in appearance due to the detonator's attacks. Thus it is very important to note that the effects caused by impulsive loadings differ with the kind of rock, namely with the nature of the rock.

Fig. 11. Results of the compression tests for marble.
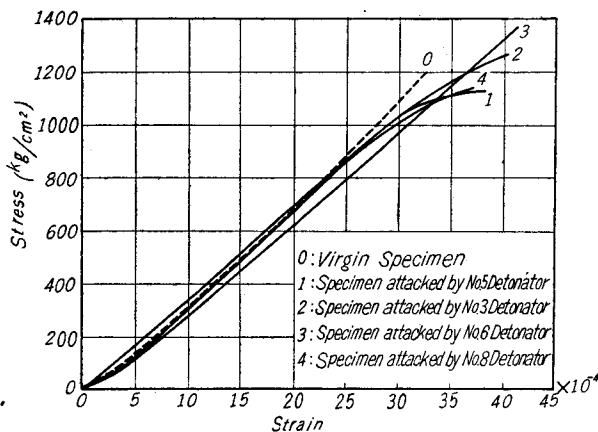
Fig. 12. Results of the compression tests for sandstone.

Stress Waves Induced in Rock Specimens Attacked by Explosives

In these cases, the experimental arrangement was somewhat different from that of the experiments using detonators as is shown in Fig. 13. A rock specimen was held between a mass of explosive and a lead block, and all of these three parts had the same diameter of 40 mm. The rock specimen and the explosive were in direct contact, but insulating paper in the form of a ring of various thickness was inserted between the rock specimen and the lead block. The moment of the arrival of the detonation wave at the upper end of the rock specimen could be measured by utilizing a special electric contact. This electric contact was composed of fine twisted insulated wires, the top of which was cut to make a tiny gap and was pushed into the lower end of the explosives as shown in Fig. 13. When the explosives were detonated, ionized gases were produced
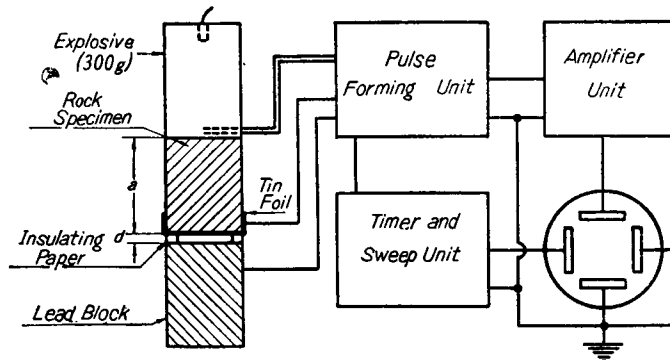

Fig. 13. General experimental arrangement.

around the gap of these insulated wires and the electric circuit was thus completed to mark a first pulse on the oscillograph. Then the moment of the arrival of the stress wave at the lower end of the rock specimen which was shown by the second pulse on the oscillograph could be detected by utilizing the other electric contact where contact was established by the forward motion of the lower free end of the rock specimen. As shown in the figure this electric contact was made by the tin foil which covered the lower end of the rock specimen and the lead block underneath it.

In this arrangement the total time required for the stress wave to propagate in the rock specimen, including the time necessary for the second electric contact to operate, was measured with various spacings set between the specimen and the lead block. Then a diagram showing the relationship between the time measured and the corresponding spacing was made. Using this diagram the time at which the spacing converged to zero was obtained and from this the velocity

of propagation of the stress wave could be calculated easily. Again, in the above diagram, the velocity of motion at the free end of the rock specimen would be indicated by the slope of the curve corresponding to the smaller values of the spacings. Consequently, the particle velocity at the lower end of the rock specimen was computed by taking half of the above velocity.

The method utilized in the present experiments to obtain the velocity is considered to be more accurate than the one used in the former experiments.

All records were again taken by using high speed cathode ray oscillograph units. In order to photograph the phenomena against time, the time base was designed to appear in every 5 μsec on the oscillograph forming a broken line.

The explosives used in these experiments were Shinkiri dynamite, Sakura dynamite, Murasaki carlit and TNT ($\varDelta = 0.95$ g/cm^3), and in every measurement 300 grams of the given explosive were used, covered with a steel tube having an inner diameter of 42 mm.

The rock specimens used were the same as those used in the former experiments except that some concrete mortar specimens were also tested in these experiments.

An example of the oscillograms is shown in Fig. 14 and of the time-spacing diagrams in Fig. 15. The results of the experiments are summarized in Table 4.
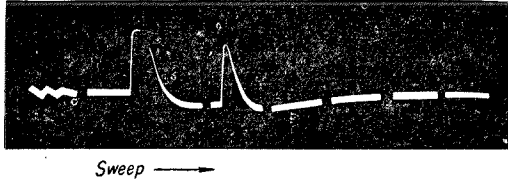

Sweep ———▶

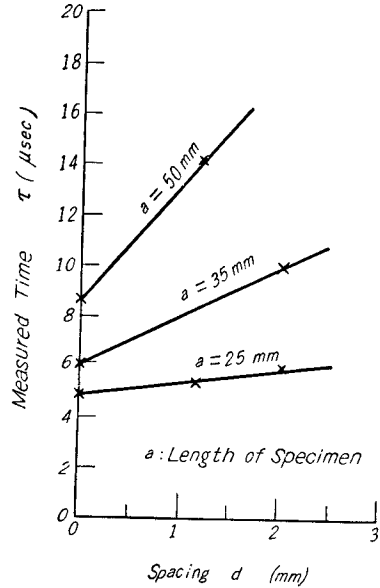Fig. 14. An example of the oscillograms.

Fig. 15. An example of time-spacing diagrams.

The propagation velocities c' of the stress wave shown in Table 4 are the mean velocities measured for each length of the specimens. Consequently, we tried to examine the local velocity c_i of the stress wave in the specimen for a particular increment by utilizing the following equation (2),

$$c_i = \frac{c_i' a_i - c_{i-1}' a_{i-1}}{a_i - a_{i-1}} \qquad i = 1, 2, 3, \cdots, n \qquad (2)$$

where c_i' is the measured velocity for a given length a_i of the specimen.

Table 4 Summarized Results of Experiments

Specimen	Explosive	Length of Specimen, a (mm)	Mean Wave Velocity in Distance a c' (m/sec)	Particle Velocity (m/sec)	Peak Pressure (kg/cm^2)
Concrete mortar ($\rho = 2.06$g/cm^3)	Sakura dynamite	20.4	3460	835	6.06×10^4
		41.1	3610	84	0.65
		61.1	3950	39	0.29
		81.0	3680	23	0.17
	Shinkiri dynamite	21.0	3750	1000	6.64
		40.0	3330	114	0.92
		60.5	3680	40	0.31
		80.1	3640	23	0.16
	Murasaki carlit	22.5	—	160	—
		60.0	3160	35	0.29
		81.9	3560	20	0.15
Marble ($\rho = 2.7$g/cm^3)	Sakura dynamite	25.2	5310	238	—
		50.0	5550	117	—
	Shinkiri dynamite	25.0	5160	1000	16.7
		35.0	5840	264	4.9
		50.0	5450	115	2.5
	Murasaki carlit	25.2	5860	209	3.16
		35.0	5800	122	0.91
		50.0	5420	72	0.76
Sandstone ($\rho = 2.6$g/cm^3)	Shinkiri dynamite	25.2	4160	1000	—
		34.0	3400	—	—
		50.0	3130	—	—
	Murasaki carlit	24.9	5360	400	—
		50.0	4270	173	—

In Fig. 16 the results thus obtained are shown in the form of a diagram showing the change of velocity against the distance from the explosion point.

In this figure we must pay attention to the fact that there exists a region showing a rather low propagation velocity in the vicinity of the explosion point. Up to this time, when a solid body was attacked by explosives, it has been recognized that the propagation velocity of the induced stress wave took its maximum value at the explosion point and decreased continuously with increase in the distance from the explosion point. However the results of these experiments are somewhat different from the traditional viewpoint described above. This phenomenon which indicated the presence of a lower velocity region close to the explosion point has appeared most clearly in the case of marble specimens
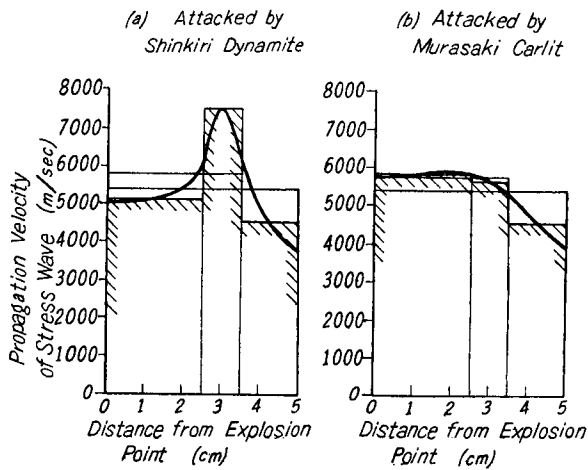
Fig. 16. Change of velocity in marble against the distance from the explosion point.

as shown in Fig. 16. Namely in these cases, the region in which the propagation velocity of the stress wave was about 5,000 m/sec continued for about 30 mm from the explosion point and then the velocity rose suddenly to about 7,000 m/sec. After that a gradual decrease of the velocity followed. All these experiments were carried out with sufficient precision[4] that the difference in the velocity measured in these experiments could not be considered as errors or mistakes. Moreover, it must be noted that these phenomena became more distinct as the intensity of the explosive increased. On the other hand, the particle velocity in this peculiar lower velocity region near the explosion point took on especially high values as shown in Table 4. As a result, an intense high pressure was attained close to the explosion point.

Generally, when a solid body is attacked by some impulsive loading, elastic waves would be induced in it for an impact velocity of about several meters per second. But with an increase in the impact velocity, plastic waves and shock waves would occur. It has already been pointed out that such changes in the forms of the stress waves accompanying impulsive loadings appeared in accordance with the impact velocities[5]. And now, when a solid body is characterized by such a stress-strain relationship as shown in Fig. 17, the propagation velocity of the stress wave induced in it can be determined by the slope of this curve,

$$c_0 = (1/\rho \cdot d\sigma/d\varepsilon)^{1/2}. \qquad (3)$$

Consequently, if we can observe the stress-strain relationship of a solid body at extremely high pressures, we can estimate the possibilities concerning whether or not a shock wave or a plastic wave can be expected in such a solid body.
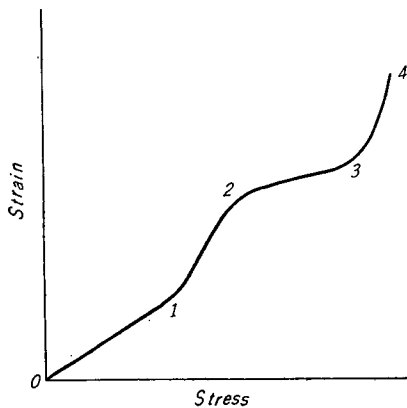

Fig. 17. A stress-strain diagram.

The compressibility $(V_0-V)/V_0$ of a solid body can be calculated approximately by using the following equations (4) and (5), provided that the values c_0 and v are previously known,

$$\sigma = 1/V_0 \cdot c_0 \cdot v \qquad (4)$$

$$v = [(\sigma-\sigma_0)(V_0-V)]^{1/2} \qquad (5)$$

where σ and σ_0 are the pressures at the back and forth of the wave respectively, while V and V_0 are the corresponding specific volumes[6].*

Consequently, the values c_0 and v obtained in these experiments were substituted in the above equations and the compressibilities corresponding to the induced stresses were computed for the specimens investigated. The results are shown in Fig. 18.

From these characteristics of rocks at the extremely high pressures indicated in this figure, it is clear that the peculiar forms of the stress waves can be more easily generated in marble specimens than in other specimens such as sandstones or concrete mortars. And in these cases the peculiar wave generated close to the explosion point was supposed to be a form of plastic wave of higher order. The fact that a high velocity region followed the above lower velocity region might also indicate the generation of a kind of shock wave. Moreover, it is

Fig. 18. Compressibility vs. stress diagram of materials tested.

interesting to note that these characteristics of rocks under impulsive high pressures are peculiar to their own physical properties and are independent of the kind of explosives used to attack them.

The relationship between the peak pressure at the wave front and the distance from the explosion point obtained in these experiments is shown in Fig. 19. As shown in the figure, the peak pressure decreased very rapidly with the distance from the point of explosion. And also, it seems to be very important from the standpoint of the explosive's effects that changes in the peak pressure with the kind of explosive used appeared only in the limited narrow range close to the point of explosion, although such conditions would vary with the brisances of
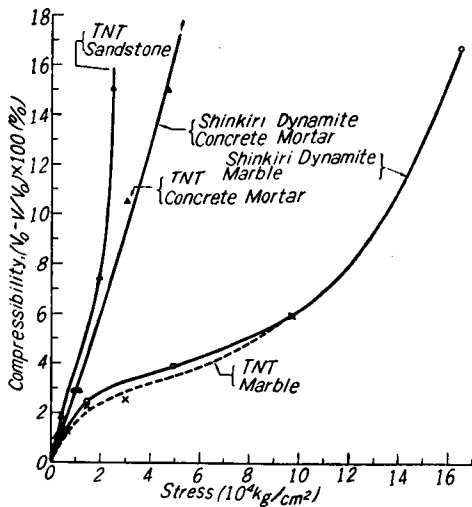
* Strictly speaking, these equations are correct theoretically only for the case of the shock wave.
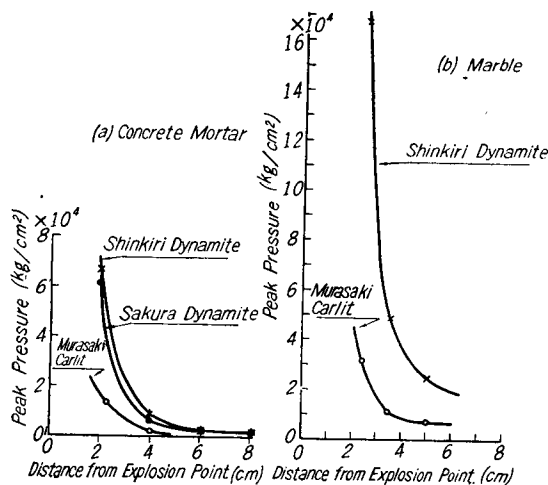
Fig. 19. Changes of peak pressure with the distance
from explosion point.

the explosives and also with the physical properties of rocks. Moreover it could be pointed out that the greater the brisance of the explosive, the higher the peak pressure attained near the explosion point.

Rock Breakages Accompanying the Shock Effects
Near the Explosion Point

When the explosives were detonated in contact with the rock specimen, it has already been stated that a form of plastic wave of higher order accompanies the plastic deformation and also that a kind of shock wave is apt to be generated close to the point of explosion. The mechanism of the rock breakage brought about with these wave motions near the explosion point may be considered as follows. Namely, in the region of the plastic wave of higher order, though it is limited only to the region no more than several tens of millimeters from the explosion point, the rocks are supposed to be decomposed partly by the extremely high temperature expected at the wave front, and then they are shattered into very fine pieces in accordance with the sudden decrease in temperature resulting from the release of the stress at the wave front. Such kinds of rock breakage are generally recognized as the breakage caused by the intense compression exhibited by the explosion gases close to the explosion point and can be practically observed near the bottom of a bore hole in which the explosives have been charged.

Shock waves generated in rocks may also cause brittle fractures with the advance of their wave fronts. However, these intense effects in breaking rocks

caused by the actions of high pressure waves, appear noticeably only in the limited region close to the point of explosion.

But we must add that the fractures caused by the reflected stress waves are excluded here in considering the problem of rock breakage.

Acknowledgments

References

1) H. Kolsky: "Stress Waves in Solids." Oxford University Press, London, p. 41 (1953)
2) J. S. Rinehart: Jour. Appl. Phys., **22.** 555 (1951)
3) H. Kolsky: Proc. Phys. Soc., London, **B62,** 693, 695 (1949)
4) T. Sakurai: Jour. Explosive Soc. Japan, **17,** 35 (1956)
5) M. P. White & C. Griffis: Jour. Appl. Mech., **19,** 256 (1948)
6) N. Yamaga: "Thermodynamics (in Japanese)," Hitotsubashi Book Co. Ltd., p. 358 (1955)